small methods
www.small-methods.com

Recent Advances in Structured Illumination Microscopy: From Fundamental Principles to AI-Enhanced Imaging

Heng Zhang, Yunqi Zhu, Luhong Jin, Haixu Yang, Jianhang Wang, Sergey Ablameyko, Xu Liu, and Yingke Xu**

Structured illumination microscopy (SIM) has emerged as a pivotal super-resolution technique in biological imaging. This review aims to introduce the fundamental principles of SIM, primarily focuses on the latest developments in super-resolution SIM imaging, such as the light illumination and modulation devices, and the image reconstruction algorithms. Additionally, the application of deep learning (DL) technology in SIM imaging is explored, which is employed to enhance image quality, accelerate imaging and reconstruction speed or replace the current image reconstruction method. Furthermore, the key evaluation metrics are proposed and discussed for assessment of deep-learning neural networks, especially for their employment in SIM. Finally, the future integration of artificial intelligence (AI) with SIM system and the perspective of smart microscope are also discussed.

1. Introduction

To acquire deep insights into the structures and behaviors of subcellular compartments, scientists have been constantly pushing the boundaries of microscopic observation to reveal the dynamic interactions underlying the vital functions of cells. Super-resolution microscopy (SRM) has revolutionized imaging techniques, which breaks the optical diffraction limit and allows for observing cellular structures with unprecedented detail.[1–4]

Among all the various SRM methods, structured illumination microscopy (SIM) has gained immense popularity in biological research due to its versatility in addressing a wide range of biological questions.[5] SIM is able to resolve structures in the 100–200 nm range, including organelles, macromolecular structures and larger complexes.[5,6] It offers several benefits when comparing with other SRM methods, for instance with improved imaging speed, and the ability to address biological questions without the need for complex sample preparation.[7] In contrast to single-molecule localization microscopy (SMLM) techniques such as stochastic optical reconstruction microscopy (STORM)[8] and photoactivation localization microscopy (PALM),[9] which sacrifice temporal resolution for spatial resolution, and stimulated emission depletion microscopy (STED),[10,11] which typically requires powerful depletion lasers, SIM has emerged as a highly desirable approach for multi-color dynamic imaging of live cells. SIM achieves a balanced compromise between temporal and spatial resolution, allowing the study of dynamic processes in living cells with minimal optical perturbation.[12–14]

The concept of SIM was first proposed by Mats Gustafsson, who realized that the resolution of conventional fluorescence microscopy could be improved by illuminating the sample with a series of stripe patterns, each shifted by a known distance. This idea was further developed by Gustafsson in the early 2000s and has since been widely adopted by researchers in the field of super-resolution microscopy.[7,15,16] SIM is performed by acquiring multiple images of the same sample under different illumination patterns, and then computationally combining these images to produce a single reconstruction with up to ~2-fold resolution enhancement. This technique has become increasingly popular in recent years due to its ability to permit multi-color live cell super-resolution imaging without the need for extensive sample preparation.[17] In addition, SIM has also been successfully combined with other imaging modalities, such as STED,[18]

H. Zhang, Y. Zhu, L. Jin, H. Yang, J. Wang, Y. Xu
Department of Biomedical Engineering
MOE Key Laboratory of Biomedical Engineering
Zhejiang Provincial Key Laboratory of Cardio-Cerebral Vascular Detection Technology and Medicinal Effectiveness Appraisal
Zhejiang University
Hangzhou 310027, China
E-mail: yingkexu@zju.edu.cn

H. Zhang, Y. Zhu, H. Yang, J. Wang, X. Liu, Y. Xu
State Key Laboratory of Extreme Photonics and Instrumentation
College of Optical Science and Engineering
Zhejiang University
Hangzhou 310027, China
E-mail: liuxu@zju.edu.cn

S. Ablameyko
National Academy of Sciences United Institute of Informatics Problems
Belarusian State University
Minsk 220070, Republic of Belarus

Y. Xu
Department of Endocrinology
Children's Hospital of Zhejiang University School of Medicine
National Clinical Research Center for Children's Health
Hangzhou 310052, China

Y. Xu
Binjiang Institute of Zhejiang University
Hangzhou 310053, China

The ORCID identification number(s) for the author(s) of this article can be found under https://doi.org/10.1002/smtd.202401616

DOI: 10.1002/smtd.202401616

Table 1. Comparison of sinusoidal SIM, Spot-scanning SIM, and Lattice SIM techniques.

Types	Variants	Advantages	Disadvantages	Refs.
Sinusoidal SIM	TIRFM-SIM, GI-SIM, Hessian-SIM, 3D-SIM, 4-beam 3D SIM, etc.	Utilizes sinusoidal light patterns to illuminate specimen, resulting in lower hardware requirements and complexity. Employs a Fourier-based reconstruction algorithm that decomposes raw images into frequency components.	Offers lower resolution and acquisition speed compared to other SIM techniques.	[58,64,67]
Spot-scanning SIM	ISM, iSIM, Airyscan, 2P-SIM, MSIM etc.	Employs a focused light beam that scans the sample point by point, allowing modulation of the spatial frequency of the illumination pattern by varying the beam focus. Uses a pixel-wise deconvolution-based reconstruction algorithm, which generally requires less computational complexity. Suitable for tissue imaging.	Requires more sophisticated hardware, including a laser source and a highly sensitive detector typically such as a photomultiplier tube (PMT).	[3,24–26]
Lattice SIM	Lattice Light Sheet, Polarization-SIM, Lattice SIM^2	Uses an array of illumination patterns (lattice) to excite multiple regions of the sample simultaneously, significantly increasing imaging speed and reducing photon-induced photobleaching. Employs a multi-frame deconvolution process for image reconstruction, allowing parallel processing of acquired data to produce high-resolution images.	Requires a more sophisticated setup, including a customized spatial light modulator and additional optical components.	[27,28]
Interferometric SIM	4Pi-SIM, I^5S I^2SIM	Uses interferometric microscopy to achieve isotropic optical resolution through interference in both the illumination and detection wavefronts, achieving 100 nm axial resolution.	More complex optical design to combine interferometric microscopy with SIM; slower imaging speed and longer data processing time	[68–70]

Light-sheet[19–22] and expansion microscopy (ExM),[23] to further enhance its imaging capabilities and increase versatility in addressing various biological problems. In this review, we aim to provide a comprehensive overview of the latest progress in SIM imaging, including the developments of its hardware and software implementations, and recent advances in deep learning techniques which have been integrated with SIM to further improve its spatiotemporal resolution and imaging quality.

2. Basic Knowledge of SIM

2.1. General Principles

By using structured patterns of light to illuminate the specimen, SIM improves spatial resolution beyond the diffraction limit. There are several variations of SIM, which include sinusoidal SIM,[5] point-scanning SIM[3,24–26] and lattice SIM[27,28] (see their comparisons in **Table 1**). The sinusoidal SIM is the most basic version of SIM that uses a sinusoidal light pattern to illuminate the specimen, creating moiré fringes that are detected by the imaging system (**Figure 1a**). Typically, a spatial light modulator (SLM)[29] or a digital micromirror device (DMD)[30] is applied to generate the structured illumination patterns, which are detected by sensitive charge-coupled device (CCD) or scientific complementary metal-oxide-semiconductor (sCMOS) camera. After the acquisition, Fourier-based reconstruction algorithm was employed to decompose these 9–15 raw images into frequency components.[31] The high-frequency information is then extracted and combined to construct a super-resolution image. sinusoidal SIM and its variations such as 3D-SIM, total internal reflection fluorescence-SIM (TIRF-SIM) etc., have been effectively applied in various biological studies.[13]

Point-scanning SIM uses a focused beam of light to sequentially scan the sample in a raster pattern (Figure 1b). By varying the beam focus, the spatial frequency of the illumination pattern can be modulated, enabling the acquisition of high-resolution data. A point-scanning SIM setup typically includes a laser source, a scanning system such as galvo mirrors to direct the light beam, and a highly sensitive detector such as a photomultiplier tube (PMT) for image acquisition. The reconstruction algorithm for point-scanning SIM is based on pixel-wise deconvolution, which combines the acquired data (the amount of the data is determined by the number of array detectors and the scanning speed) to produce a high-resolution image.[32,33] Compared to sinusoidal SIM, this method generally requires less computational complexity and has been used to visualize deep insight into tissues.[34,35] To further overcome the inherent speed limitations of point-scanning SIM, researchers developed multi-focal structured illumination microscopy (MSIM). It employs DMD to simultaneously generate multiple spots of illumination across the specimen plane. MSIM achieves

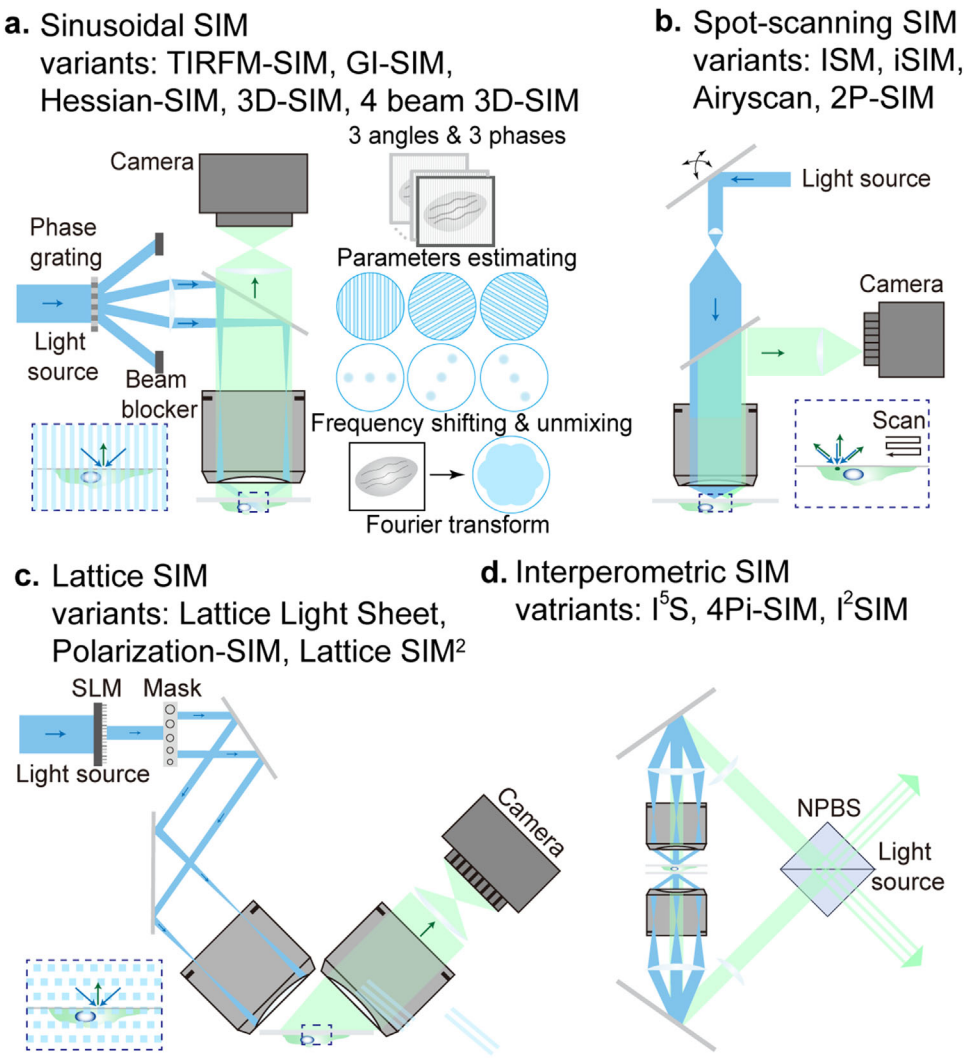

Figure 1. Conceptual diagram of sinusoidal SIM, spot-scanning SIM and lattice SIM. a) Diagram of sinusoidal SIM acquisition and reconstruction process. Periodic interference fringes are introduced on the surface of the sample after the light source is reflected by the phase grating (left). By adjusting the phase and angle of the interference fringes, typically 9 raw images are obtained for further frequency unmix to obtain a super-resolution image (right). b) The spot-scanning SIM is based on pixel-wise deconvolution, which combines the acquired data to produce a super-resolution image. The resolution point spread function (PSF) of the system is related to the excitation PSF and the emission PSF. c) Lattice SIM and its variants. A mask is added in the optical path to form lattice light spots that illuminate the sample. A specific reconstruction algorithm is used to recover one high-resolution image. Abbreviations: GI-SIM (grazing incidence SIM), ISM (image scanning microscopy), iSIM (instant SIM), 2P-SIM (two-photon SIM). d) Interferometric SIM and its variants. A dual-objective-lens interferometric system enables a near-isotropic resolution of ≈100 nm in all three dimensions. Especially 4Pi-SIM is able to achieve live-cell imaging.

significantly enhanced imaging throughput than point-scanning SIM.[36]

Lattice SIM is an advanced version of SIM that uses an array of illumination patterns (lattice) to excite multiple regions of the sample simultaneously (Figure 1c). This approach significantly increases imaging speed and induces less photobleaching than traditional sinusoidal excitation. Lattice SIM requires a more sophisticated setup, including a customized SLM and additional optical components to shape the lattice pattern. As for image reconstruction, lattice SIM involves a multi-frame deconvolution process that processes the acquired data in parallel to produce a high-resolution image.[28] Lattice SIM has been used for high-speed live-cell imaging, such as in investigating the excitatory and inhibitory synapses.[37]

It should be noted that each SIM variant comes with unique advantages in terms of hardware requirements and reconstruction algorithms (see Table 1). While sinusoidal SIM is the most widely used form, point scanning and lattice SIM offer more advanced imaging capabilities and faster acquisition speed. The choice of the appropriate SIM technique is determined by the specific requirements of the imaging experiment, including sample properties, resolution requirements, and acquisition speed.

2.2. Structured Illumination Devices and Image Reconstruction Algorithms

2.2.1. Hardware Developments

The most important part of hardware development lies in the light illumination and modulation devices for SIM imaging. These developments enable for imaging with improved temporal resolution, deep light penetration depth, reduced phototoxicity, and enhanced spatial resolution.

SLM and DMD are the two major devices used to implement the SIM illumination pattern. SLM is a transmissive modulator that uses liquid crystal materials to modulate the phase and amplitude of incident light, while DMD is a reflective modulator that uses microelectromechanical systems (MEMS) technology to manipulate incident light through an array of micromirrors.[38] Recent advances in both technologies have led to improvements in SIM performance. New liquid crystal on silicon (LCoS) SLMs offer increased pixel density, faster response time and wider modulation range[39,40] In parallel, DMD technology has seen advances in miniaturization and integration, resulting in more compact and versatile systems.[41]

Random illumination SIM, also known as blind-SIM, is a promising new technique for improving SIM performance by exploiting non-periodic structured illumination.[42–44] By incorporating a random phase mask into the optical path, multiple random illumination patterns can be generated, offering several advantages over traditional SIM methods. A key benefit of random illumination is the reduction of photon damage to the sample, as even distribution of light intensity across the sample minimizes the risk of photobleaching and phototoxicity. In addition, the non-periodic nature of the illumination patterns reduces specimen-induced aberrations, enabling deeper tissue imaging.[45] Furthermore, random illumination simplifies the optical system by eliminating the need for complex pattern generation and synchronization, making it more accessible and cost-effective.

In addition, lattice SIM^2, an advanced SIM technology that surpasses its predecessor Lattice SIM has been commercialized. By using phase masks and diffraction gratings, Lattice SIM^2 optimizes the lattice illumination pattern and achieves improved resolution beyond the capabilities of Lattice SIM.[46–48] Lattice SIM^2 represents a significant advancement, offering improved resolution, faster imaging speed, and an expanded range of applications. However, Lattice SIM^2 has limitations, such as sensitivity to sample movement, dependence on sample quality, and high maintenance costs.

2.2.2. Development on SIM Reconstruction Algorithms

Over the years, various SIM reconstruction methods have been developed to improve the quality and efficiency of reconstructed images (summarized in **Table 2**). Among these methods, efforts have been paid to improve either the quality or the speed of image reconstruction, which represent significant advances in the field.[31,49–51]

Spatial domain methods for SIM reconstruction directly manipulate the raw images in the spatial domain, without the need for Fourier transformations.[52] This kind of method provides improved performance in noise suppression and artifact reduction. However, spatial domain methods commonly suffer from increased computational complexity compared to frequency domain methods, which analyzes the frequency domain of the original images and identify the common frequency components in order to reduce the amount of raw data required. The optical transfer function (OTF) describes the response of an imaging system to different spatial frequencies. OTF correction methods aim to improve the quality of the reconstruction by taking the aberrations and distortions of the imaging system into account. These methods, such as high-fidelity SIM (HiFi-SIM),[53] joint space frequency reconstruction-based SIM (JSFR-SIM)[54] and joint space frequency reconstruction-based artifact reduction algorithm SIM (JSFR-AR-SIM),[55] provide more accurate reconstruction results. HiFi-SIM improves image reconstruction and reduces artifacts while achieving higher spatial resolution and noise suppression.[53] JSFR-SIM combines system optimization with Fourier ring correlation for improved image quality and resolution assessment,[54] while its extension, JSFR-AR-SIM, incorporates HiFi- and JSFR-SIM to further enhance image reconstruction speed and to reduce artifacts.[55] Besides, physical-based background filtering SIM (BF-SIM)[56] functions to remove the background of raw images and enhance resolution through different SIM reconstruction algorithms. However, the need for accurate OTF measurements or physical models proposal may limit their applicability in some situations. Besides, dCOR-SIM (dichotomy–correlation SIM)[57] innovatively refines OTF correction by employing a dichotomy strategy to estimate illumination parameters rapidly and accurately. This approach minimizes the iterative processes of conventional methods, thereby accelerates high-quality super-resolution imaging and reduces artifacts while maintaining robustness to noise. Sparse deconvolution algorithms exploit the sparsity and continuity of biological samples to achieve higher resolution than traditional SIM reconstruction methods.[58,59] These algorithms reduce noise and can be applied to live-cell imaging, allowing the study of dynamic cellular processes at high spatial and temporal resolution. Nonetheless, these techniques have certain drawbacks, such as high computational complexity and the need for time-consuming manual optimization of various parameters.

A major challenge with SIM is the requirement of multiple raw images to achieve super-resolution, which can be time consuming and limit the temporal resolution of the technique. Several methods have been developed to reduce the number of raw images required for reconstruction.[60–63] These can significantly improve the temporal resolution of SIM, but at the same time may potentially introduce artifacts or compromise resolution in some circumstances. grazing incidence SIM (GI-SIM), by innovative combination of structured illumination and grazing incidence illumination, has enabled high-resolution imaging of surface structures such as cell membrane and surface-associated proteins.[64] GI-SIM is a promising super-resolution technique for imaging surface features, as it utilizes highly inclined and laminated optical sheet (HILO)[65] microscopy and with slide window reconstruction algorithms. Specifically, the slide window reconstruction algorithm uses 1–3 angles for the first

Table 2. Comparison of different non-DL SIM reconstruction algorithms.

Types	Instances	Advantages	Disadvantages	Refs.
Spatial domain reconstruction	SP-SIM, etc.	Directly manipulate raw images in the spatial domain, eliminating the need for Fourier transformations. Provide improved performance in terms of noise suppression and artifact reduction.	Increased computational complexity compared to frequency domain methods.	[52]
OTF correction	HiFi-SIM, JSFR-SIM, JSFR-AR-SIM, BF-SIM, dCOR-SIM, etc.	Improve the quality of the reconstruction by accounting for the aberrations and distortions of the imaging system. Provide more accurate reconstructions, improved image quality, resolution enhancement, and artifact reduction.	The need for accurate OTF measurements or physical models may limit their applicability.	[53–57]
Reducing raw images	7-frame SIM, SF-SIM etc.	Reduce the number of raw images required for super-resolution, improving the temporal resolution of SIM.	May introduce artifacts or compromise resolution in some cases.	[60–63]
Slide-window reconstruction	GI-SIM, etc.	Enables high-resolution imaging of surface structures. Utilizes highly inclined and laminated optical sheet (HILO) microscopy with slide window reconstruction algorithms, resulting in faster temporal resolution.	More computationally intensive due to the slide window reconstruction algorithm.	[64]
Sparse deconvolution	Sparse-SIM, etc.	Exploit the sparsity and continuity of biological samples to achieve higher resolution. Reduce noise and can be applied to live-cell imaging.	High computational complexity and the need for time-consuming manual optimization of various parameters.	[58,59]

high-resolution frame and 2–4 angles for subsequent frames, resulting in almost three times faster temporal resolution than traditional SIM setups.

In summary, spatial domain methods can provide better noise suppression and artifact reduction, but can be computationally expensive. OTF correction methods can improve reconstruction accuracy, yet require accurate OTF measurements. Reducing raw data requirements for reconstruction can improve temporal resolution, but may introduce artifacts and compromise resolution. The slide-window based reconstruction on GI-SIM provides better reconstruction with accelerated speed, however it can be more computationally intensive. The sparse deconvolution algorithms can provide higher resolution and contrast, while may require advanced optimization techniques and longer processing time. Therefore, further research is still needed to optimize and combine these methods for specific applications that would further advance the field of SIM reconstruction.

2.2.3. Application of Advanced SIM in Biology

Spatial resolution, temporal resolution and light exposure are the three primary trade-offs that limit the performance of fluorescence microscopy imaging.[66] Recently, there have been a surge in publications focusing on optimization of reconstruction algorithms and developing suitable devices for live cell SIM imaging with high spatiaotemporal resolution. For instance, leveraging prior knowledge of the sparsity and continuity of biological structures, sparse deconvolution algorithms have been developed to enhance the lateral resolution of images.[59] Although electron-multiplying charge-coupled device (EMCCD) cameras offers superior electron multiplication gain and quantum efficiency, their large pixel size still restricts system resolution. However, sparse deconvolution can extend the OTF of the system, allowing for the visualization of previously indistinguishable ring-like endoplasmic reticulum (ER) tubules (**Figure 2a**). The four-beam 3D-SIM technique, which positions a mirror directly opposite to the sample, facilitates four-beam interference with higher spatial frequency content than conventional 3D-SIM illumination.[67] This results in near-isotropic imaging with ≈120 nm lateral and 160 nm axial resolution. Wide-field imaging of fixed U2OS cells immunolabelled for Tomm20, a marker for the outer mitochondrial membrane, failed to resolve the inner mitochondrial space. In contrast, both 3D-SIM and four-beam SIM provided lateral views in which the mitochondria cristae were easily discernible. However, only four-beam SIM could reliably resolve the inner spaces in axial view (Figure 2b). Recent advances in SIM have achieved isotropic 3D resolution by integrating interferometric

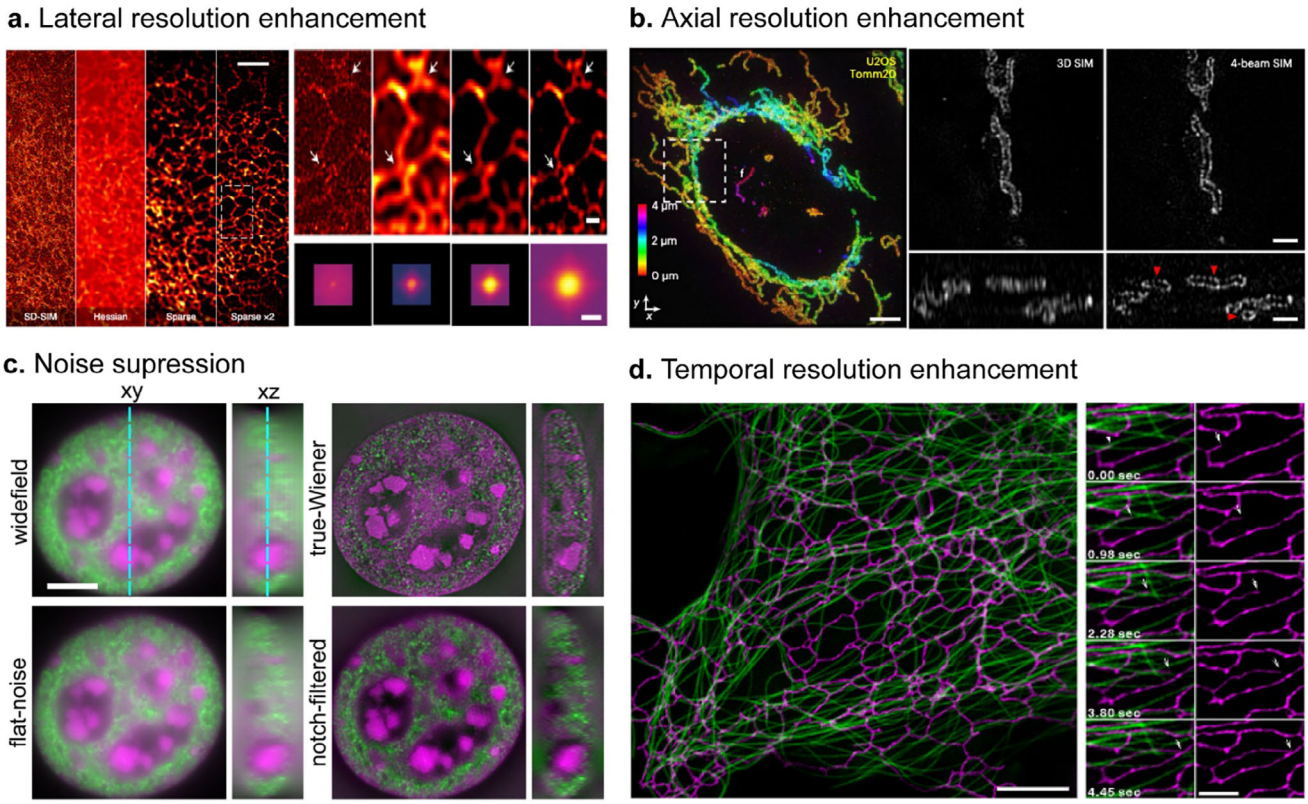

Figure 2. Application of advanced SIM in biology. a) Lateral resolution enhancement achieved by sparse deconvolution. Comparison of the endoplasmic reticulum (ER) tubules imaged via SD-SIM, Hessian, Sparse and Sparse × 2 (left). Enlarged regions for four methods (right top) and the corresponding Fourier Ring Correlation (FRC) map (right bottom). The FRC resolution of SD-SIM images is ≈195 nm, while the Sparse×2 deconvolution image is artificially upsampled to two-fold, resulting in an increased FRC resolution of ≈102 nm.[59] Reproduced with permission.[59] Copyright 2022, Springer Nature. b) Four-beam 3D-SIM achieves isotropic super-resolution imaging of Tom20 labeled mitochondria. Color-coded depth image of a U2OS cell (left) and enlarged xy, yz view of the white box in left (right). Four-beam 3D-SIM improves lateral resolution compared with regular 3D-SIM.[67] Reproduced with permission.[67] Copyright 2023, Springer Nature. c) Demonstration of different reconstruction algorithms in suppressing the noise of a mouse C127 cell.[71] Reproduced with permission.[71] Copyright 2021, Springer Nature. d) GI-SIM visualizes the long-term ER-MT dynamic interactions.[64] Reproduced with permission.[64] Copyright 2018, Cell. Scale bars (from left to right, top to bottom): 5 µm, 5 µm, 500 nm (a); 4 µm, 1 µm, 1 µm (b); 5 µm (c); 5 µm, 2 µm (d).

microscopy techniques that provide exceptional axial resolution (≈100 nm). Representative developments in this area include 4Pi-SIM,[68] I^5S,[69] and the more recent I^2SIM[70] (Figure 1d and Table 1). Notably, 4Pi-SIM has demonstrated the capability for live-cell imaging while maintaining this enhanced 3D resolution.

Reconstruction algorithms play a crucial role in regulating the quality of reconstructed image to achieve noise-controlled outcomes. True-Wiener-filtered SIM optimizes contrast across different signal-to-noise ratios (SNRs), while flat-noise SIM effectively mitigates structured noise artifact to preserve resolution.[71] Both methods eliminate user-adjustable reconstruction parameters, relying instead on physical parameters to maintain objectivity. The notch-filtered SIM reveals a trade-off between contrast and the appearance of natural noise, which can be partially addressed through further notch filtering, though at the expense of decreased SNR. Representative images of widefield and noise-controlled SIM reconstruction of a mouse C127 cell were illustrated in Figure 2c.[71] Furthermore, advancements in GI-SIM have demonstrated the ability to visualize dynamic events near the cell cortex with 97 nm resolution and a temporal resolution of 266 frames per second.[64] This technique has been employed to characterize endoplasmic reticulum and microtubule (ER-MT) interactions and to investigate the underlying mechanisms of ER network reorganization (Figure 2d). Collectively, these advances in SIM enhance live cell imaging by elevating both lateral and axial resolution, suppressing noise, and increasing temporal resolution.

3. Application of Deep Learning Methods to Enhance SIM Performance

Deep learning (DL) is a machine learning technique that utilizes learnable models with well-designed structures to extract complex feature from data and accomplish specific tasks. In recent years, many deep learning-based methods have been applied to SIM. In this section, we will briefly introduce the fundamentals of deep learning, focusing specifically on the common neural networks used in SIM applications (**Figure** 3a–c) and a comparison with conventional approach (Figure 3d). We will categorize those methods into four categories (**Figure** 4a–c), describe their

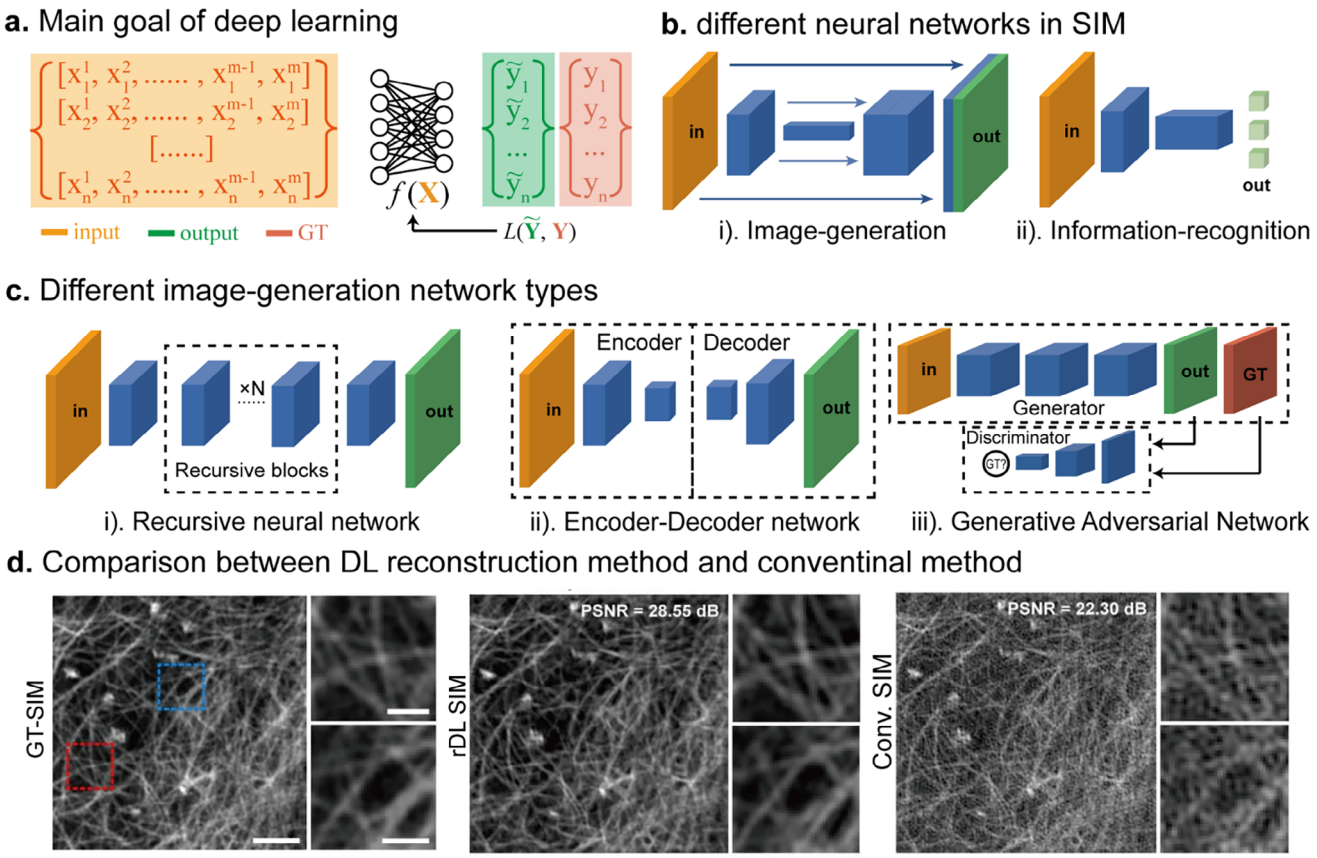

Figure 3. Commonly used deep learning models for SIM imaging. a) Deep learning methods minimize the objective function $\mathscr{L}$ to uncover hidden patterns in large datasets. b) Two types of neural networks commonly used in SIM: i) image-generation networks (producing images for tasks such as segmentation, super-resolution reconstruction, and image deconvolution) and ii) information-reconstruction networks (extracting high-level semantic information for tasks). c) Three types of image-generation networks: i) encoder-decoder networks[77–83] (using an encoder to extract information and a decoder to reconstruct images), ii) generative adversarial networks[79,84–88] (with a generator and discriminator trained concurrently), iii) physically constrained networks[74,89–91] (incorporating physical constraints to enforce adherence to known physical principles during training and inference). d) Comparison of SR reconstruction performance between deep learning[74] and conventional algorithms on noisy F-actin images. The PSNR values are indicated at the top-right corner of each image. The results demonstrate that the deep learning method exhibits superior noise robustness and effectively suppresses reconstruction artifacts compared to the conventional approach. Reproduced with permission.[74] Copyright 2022, Springer Nature.

principles, and provide representative examples. Finally, we will discuss the criteria for evaluation the performance of DL methods in practicle applications (Figure 4d–h).

3.1. Fundamentals of Deep Learning

The aim of deep learning is to learn and extract useful feature representations from large datasets by building models with efficiency and accuracy. The typical workflow of deep learning is illustrated in Figure 3a. Commonly, supervised learning is employed to tackle most deep learning tasks, which requires a substantial amount of input-ground truth (GT) data pairs. During the training stage, the objective function (represented as function $\mathscr{L}$ in Figure 3a) is minimized to ensure that the distance between model outputs $\hat{Y}$ and the GT Y will close enough to each other. Through repeated iterations, a deep learning model with stable output ($\mathscr{L}$ remains relatively constant across iterations) can be achieved. In addition to supervised learning, alternative learning approaches are applicable under different conditions. For instance, weakly supervised learning can be used when only a portion of the data has associated GT. It has been utilized for organelle segmentation in various types of microscopic images.[72,73] Alternatively, unsupervised learning or self-supervised learning can be applied to unlabeled dataset to directly explore the internal structure or rules inherent in the original data, or to generate virtual labels to facilitate the training process.[67,74]

To address a variety of image processing tasks, researchers need to choose different types of neural networks. Two types of neural networks are widely utilized in SIM-related applications (Figure 3b): i) image-generation networks, such as U-Net,[75] residual channel attention networks (RCAN),[76] etc., which are suitable for SIM super-resolution reconstruction, fluorescence structure segmentation, cross-modality imaging and other similar image-generating tasks; ii) information-recognition networks, which are effective for image classification, object detection, among others.

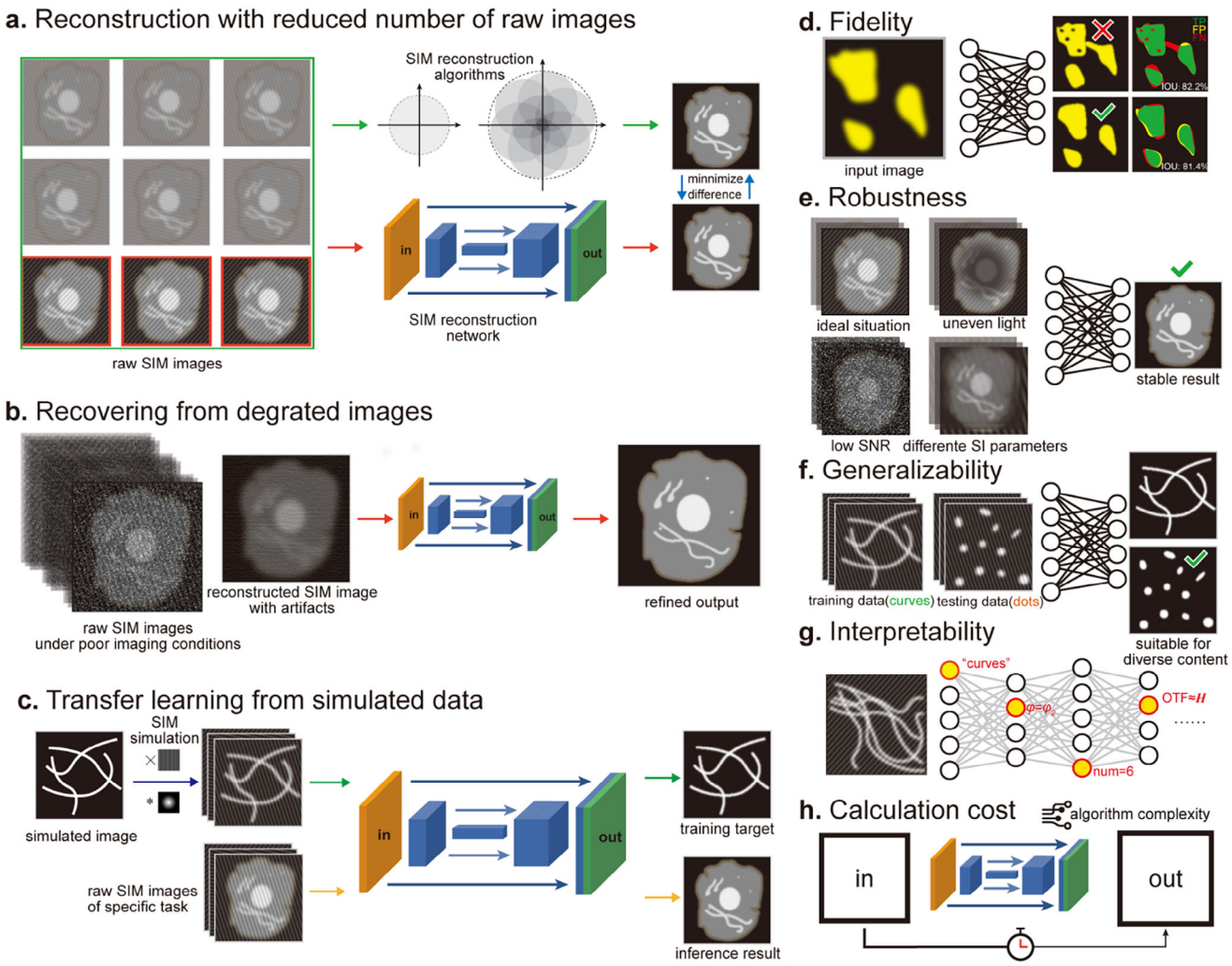

Figure 4. Applications of deep learning to enhance SIM imaging (a–d) and important metrics for evaluation of model performance (e–i). a) Reducing the number of SIM raw images to accelerate reconstruction.[84,95] b) Reconstructing raw images acquired under poor SNR conditions, or removing artifacts from the reconstructed images.[80,81,86,102–104] c) Transfer learning from abundant accessible data,[107] followed by fine-tuning for specific tasks. Evaluation criteria for deep learning models: d) Fidelity: The ability to avoid image distortion and precisely extract important information. e) Robustness: Maintaining performance under various perturbations. f) Generalizability: Making correct predictions on unseen data. g) Interpretability: The extent to which a model's decision-making process can be understood and explained in human terms. h) Calculation cost: Consumption of resources for inference and training.

There are three commonly used types of image-generation networks (Figure 3c): i) Encoder-Decoder network, such as U-Net, have been widely used in biological imaging, including SIM.[77–83] This type of network extracts features from input images using an encoder, where the feature map typically decreases with increasing network depth as the number of channels increases. Subsequently, the decoder generates output images based on those features obtained from the encoder. ii) Generative adversarial networks (GANs), typically comprise of two simultaneously trained networks: a generator and a discriminator. The generator aims to create realistic images, while the discriminator tries to differentiate between real and generated images. These two networks engage in a competitive process, continually improving until the generator can produce highly realistic images.[79,84–88] iii) Physically constrained networks. This category of networks integrate physical models to enforce constraints during the network's convergence process.[74,89–91] In the context of deep learning-based SIM, researchers have leveraged prior knowledge such as illumination patterns and point spread functions to introduce constraints or additional objective functions, thereby enhancing the model's performance during both training and inference phases.

3.2. Deep Learning Reduces Raw Image Requirement for SIM Reconstruction

To recover high-frequency information in microscopic images, the sinusoidal SIM reconstruction algorithm typically requires nine or more raw images. A few studies have demonstrated

SR image reconstruction using fewer than nine raw SIM images,[52,60,92,93] but these approaches may require extra computational complexity and struggle to outperform the traditional method. In contrast, deep learning methods offer solutions that can reduce the number of input images while achieving comparable or even superior performance. Specifically, deep learning methods enable convenient task-specific reconstruction processes with fewer input images, leading to higher efficiency in data acquisition and processing. For instance, Ling et al. used cycle-consistent generative adversarial networks (cycleGANs)[94] to achieve super-resolution reconstruction of sinusoidal SIM and nonlinear SIM (NSIM) using structured light images in only one direction, thanks to the isotropy of the fluorescence group (Figure 4a).[84,95] Similarly, Chen et al. introduced an additional frequency domain loss during the training of conditional generative adversarial networks (cGANs)[96] to achieve super-resolution reconstruction of both 2D- and 3D-SIM using only one image per direction.[88]

More recently, researchers have utilized single-frame structured light images to enhance the resolution of wide-field microscopy. They proposed two different deep learning-based approaches to achieve this goal. Zhang et al. designed a five-way GAN network to generate the original structured light images, followed by a super-resolution reconstruction network using a 6-input and single-output deformation of U-Net (DU-Net).[79] Meanwhile, Cheng et al. developed the fast and lightweight SIM super-resolution network (FLSN), which comprises multi-scale networks, a noise estimator, and bandpass attention modules.[97] These approaches not only significantly reduce the time required for SIM image acquisition but also mitigate the effects of phototoxicity and photobleaching on fluorescent samples.

Despite the efficiency and effectiveness of deep learning methods for image analysis, there are limitations to their applicability. A key concern is the generalizability of deep learning networks, which require diverse datasets for training. For example, Zhang et al. noted that their neural network is only applicable to images with similar structure to those in training data, which restricts the portability and versatility of these methods.[79]

3.3. Deep Learning Enhances Image Quality for SIM Reconstruction

During microscopic imaging, particularly when observing live-cell samples, the conditions for acquiring high-quality images can be severely limited. Capturing live cells under intense illumination poses a significant challenge due to their susceptibility to light-induced photobleaching and cellular photodamage. As a result, the reconstruction of SIM images often suffers from diminished quality and is susceptible to artifacts. To enable sustained long-term imaging, it is common practice to reduce light intensity. However, this would significantly deteriorate the SNR of the raw data. In addition to low SNR, uneven light field distribution and low structured light modulation depth can further impede accurate SIM reconstruction.

Conventional image denoising algorithms, such as Wiener filter, have been widely used to improve noisy microscopy images.[98,99] Additionally, deconvolution methods, for instance Richardson-Lucy deconvolution (RLD),[100,101] have shown to effectively enhance fluorescence image quality.[55,74] However, many of these methods require an extended and iterative process, as well as sophisticated parameter optimization. In contrast, deep-learning networks can achieve strong denoising results without extensive parameter adjustments.[81] They have been applied to perform end-to-end high-resolution reconstruction under low light illumination conditions (Figure 4b)[80,81,86,102–104] by leveraging the feature extraction capabilities of the neural networks. Researchers have also utilized self-supervised deep learning methods to denoise SIM images using only noisy inputs,[105] significantly reducing the burden of large training data preparation. Moreover, deep learning methods can overcome hardware-related resolution limitations. For example, researches have used carefully aligned images captured from lenses with varying numerical aperture values to train a resolution-enhancement model, enabling high-resolution imaging in a wider field of view (FOV).[85] Similarly, wide-field (WF) or total internal reflection fluorescent (TIRF) microscopy require less complicated hardware compared to SIM. By using a WF-SIM data pair, neural networks can learn the conversion between these two images to achieve resolution improvement.[85,106] In this process, the data-driven neural networks function as a deconvolution algorithm, but with fewer parameter tuning challenges compared to traditional methods. Additionally, Li et al. managed to train an isotropization network on original 3D-SIM images with low SNR using a self-supervised approach, achieving isotropic high-quality 3D-SIM images.[67]

3.4. Deep Learning Achieves Experimental-Data-Free SIM Reconstruction through Physical Modeling

Most deep learning approaches typically require paired SIM and WF microscopy datasets during model training – a paradigm known as supervised learning. However, such approaches often face practical challenges in biological imaging applications, particularly regarding the acquisition of high-quality paired datasets from delicate biological specimens. To address this limitation, researchers are increasingly adopting synergistic strategies that combine simulated data generation with transfer learning techniques.

Transfer learning is a promising approach to address the challenge of insufficient training data in deep learning,[107] which otherwise may induce overfitting or underfitting. The core concept of transfer learning involves pre-training models on large datasets that are similar to the target task, followed by fine-tuning with limited data specific to that task (Figure 4c). This method has been applied to SIM to accelerate the image reconstruction process. Christensen et al. proposed ML-SIM (machine learning-SIM),[108] which used the high-resolution images from the DIV2K dataset[109] and generated SIM data pairs by simulating the SIM imaging process in silico. They trained these data pairs using the RCAN network[76] and found that the optimized network exhibited better robustness and artifact resistance on real microscopic data compared to traditional open-source SIM reconstruction approaches.[108,110] Similarly, Luo et al. used synthetic data, such as dots and lines resembling content found in fluorescent microscopic images, and simulated the SIM imaging process for training, which yielded comparable results to

ML-SIM.[77] Additionally, by integrating transfer learning with fine-tuning, similar tasks become easier to learn, which promotes the emergence of highly generalized DL-based SIM processing networks.

3.5. Evaluation the Performance of Deep Learning Networks

Evaluation metrics play a crucial role in providing the benchmark for optimization of deep learning algorithms. In this section, we will introduce five widely used evaluation metrics from various perspectives to assist in assessing SIM-related deep learning models.

3.5.1. Fidelity

After training, the deep learning model needs to be evaluated from various aspects to ensure its effectiveness. First is to verify whether the output images matches the input without irrelevant hallucinations or severe distortion (as shown in Figure 4d). To ensure and improve the fidelity of the model, researchers can guide the optimization direction of the model by including global or structural loss functions, such as SSIM loss[67,74,85,88,91,102,111] or frequency domain loss.[77,88,112] In some circumstances, adversarial training modes, such as GANs[113] and its derivatives cGANs and cycleGANs, are employed. These methods utilize discriminators to keep the generator's output close to GT.[79,85,86,88,106] Previous studies have demonstrated that using a discriminator is more effective than using only U-Net for preventing the generation of fake information.[114] Moreover, it is important to synthesize the results of multiple metrics during testing to obtain a comprehensive evaluation of the model. However, if only one metric, such as the intersection over union (IoU), is used to compare the performance, which may lead to false conclusion as shown in Figure 4d, where the lower row shows significantly better results than the upper row (with less distortion). Thus, applying appropriate constraints during training and using multiple metrics during testing can both contribute to maintain the fidelity of the deep learning models.

3.5.2. Robustness

Robustness is another critical metric for assessing model performance (as illustrated in Figure 4e). It refers to the ability of the model to resist small perturbations that occur in input data. The robustness of the model applied to SIM images is reflected in its capability to reconstruct stable, high-resolution, high-quality images even when using raw images with low SNR, inhomogeneous light fields, unstable or differently parameterized structured light, etc. The choice of loss function significantly impacts the robustness of the trained model in SIM applications. Regularization techniques,[115] such as total variation (TV) loss,[89] are commonly employed to improve the model's resilience, particularly under low SNR conditions. In addition to the above mentioned deep learning assisted SIM image denoising, certain DL-based SIM methods have demonstrated strong noise resistance during testing, even without purposely designing the denoising module (e.g., using low-high SNR data pairs, special loss components, and uniquely designed network structure).[85,91] On the other hand, traditional SIM has higher demands for SNR and light illuminating conditions for the raw images and is prone to produce artifacts[116] (see comparison in Figure 3d). Given the data-driven nature of deep learning, it is crucial for researchers to acquire sufficient amount of perturbation-containing data for network training to ensure its robustness. In scenarios where well-matched data pairs are difficult to obtain, studies have demonstrated that using self-supervised methods[74,89,117] or adding artificial simulated perturbations[77,82] can improve the network's resistance to the input disturbances.

3.5.3. Generalizability

Generalizability refers to the ability of a DL model to provide accurate predictions or outputs on unseen data (Figure 4f). As mentioned earlier, most deep learning networks are data-driven, meaning they can only output reliable results for a specific type of data. In applications requiring high model generalizability, such as super-resolution imaging of cells with a large variety of morphologically different organelles, the most straightforward approach is to collect sufficient raw of each organelle type for simultaneous training. However, this approach requires complicated experimental steps and different methods for labeling and acquiring each subcellular structure. Alternatively, one can use simulated data,[77,108] or pre-train the network on simulated data and then fine-tune it with real data. Simulated data are easily obtainable and can be tailored to include specific geometric characteristics necessary for the tasks.

3.5.4. Interpretability

Interpretability or explainability is another metric that has been frequently mentioned in recent years to measure the transparency of machine learning mechanisms. It reflects the DL model's ability to provide understandable structures and predictable, controllable outputs during the inference stage (Figure 4g).[74,97,118,119] Interpretable networks not only help researchers grasp the underlying mechanisms of model operation but also often reduce redundant components, resulting in lighter models.[97] By transforming traditional image processing methods, which may contain iterative algorithms into structure-specific neural networks, more efficient and lightweight interpretable networks can be constructed.

Another effective method for enhancing the comprehension of the DL-SIM model is utilizing of uncertainty maps. For instance, Zhu et al. utilized a Bayesian convolutional neural network to quantify the uncertainty of the SIM reconstruction network.[82] The resulting heat map serves as a reliable reference for the predictions of the reconstruction network, indicating the confidence level in the results.

3.5.5. Complexity

The computational complexity of neural networks is also of great significance for applications (Figure 4h). It typically includes four

aspects: 1) Floating point operations (FLOPs), which refers to how many basic floating point operations the network needs to perform during inference or training. Lower FLOPs often allow the network to run on a wider range of hardware platforms, and consuming less computation time; 2) Number of parameters in the network. In general, more parameters can bring stronger expressive power (as seen in deeper U-Net), but it increases the risk of overfitting. Researchers have to ensure that the model is complex enough to adapt to actual tasks, and avoiding to add unnecessary parameters; 3) Memory access, which refers to how much memory the network costs during calculation. This is mainly determined by the size of the model and the size of the input image. Practically, researchers need to reasonably limit the architecture of the neural network according to the image size to prevent excessive consumption of memory during training and testing; 4) Latency, which refers to the total time taken between input and output. For tasks that require real-time inference, such as super-resolution reconstruction and high-throughput image analysis, if the network latency is higher than the data acquisition time, it may not meet the real-time requirements. Methods to reduce latency include using simplified network architectures, selecting optimal hardware configurations, and employing model pruning and quantization.

In recent years, studies have examined the impact of neural network complexity on SIM image processing, and have efficiently completed specific tasks through self-designed lightweight neural networks.[97] Notably, some researchers have employed a strategy called zero-shot learning, enabling the neural network to perform image reconstruction and high-resolution deconvolution under various structured light patterns through multiple iterations based solely on physical constraint equations, with no need for training.[89,91] Although traditional network architectures are still used, this unique computational strategy does not require large-scale data support or complex and lengthy training procedures. We believe that emerging deep learning technologies such as zero-shot will play an increasingly significant role in SIM imaging.

4. Conclusion and Outlooking

Substantial progresses have been made in the field of SIM over the past few years, which have led to imaging with high speed, enhanced image quality, and reduced complexity for subsequent image reconstruction. With the advent of open-SIM[120] add-on modules, conventional microscopes can be easily upgraded to a super-resolution SIM setup. Concurrently, advancements in SIM hardware have introduced innovative illumination patterns, such as random illumination[43,44] and lattice light,[46,47] all of which have diversified the structured light used in SIM, making it more adaptable to various biological needs. Novel reconstruction algorithms, such as JSFR-SIM[54] and Sparse-SIM,[59] have enabled SIM reconstruction to operate effectively with lower illumination doses, weaker SNR, and higher temporal resolution while maintaining spatial resolution. Moreover, the application of deep learning in SIM has accelerated reconstruction speed by utilizing fewer raw images[84,88,95] and even replaced the reconstruction process,[108,121] enabling low light illumination,[80] large field of view,[85] and isotropic-SIM imaging.[67] These developments demonstrate that DL models of image-generation type have vast potential applications in SIM. As deep learning continues to evolve, diverse model architectures will be proposed for various tasks. For instance, transformer-based structures, known for their ability to capture long-range dependencies, present a promising alternative to CNNs that are largely constrained by local receptive fields.[112,122–124] It is conceivable that DL models will also be integrated into SIM system for real-time parameter estimation[51] and optical correction,[125] thereby enhancing imaging quality and stability.

Looking ahead, several promising trends are emerging in SIM technology, including event-trigger,[78,126] content-rich,[127–129] module-diverse,[130,131] label-free[132,133] techniques, alongside the establishment of high-quality SIM image databases.[102,134] Any increase in spatial resolution often comes at the cost of longer exposure time, acquisition duration, and phototoxic damage to the biological samples. Therefore, event-trigger SIM aims to overcome this limitation by switching imaging modalities based on regions of interest, employing low-resolution (WF) observation for global views and high-resolution (SIM) for localized areas of interest.[78] Content-rich SIM seeks to extract more information from microscopic images, such as integrating fluorescence microscopy with force measurements, electrophysiological parameters, or mass spectrometry information.[127] This approach can serve as a complementary method for refining event-triggered microscopy systems. There is a growing need for module-diverse SIM systems that offer flexible and modular extensions, such as optical tweezers, microinjection devices, or laser ablation systems.[130] These innovations will significantly lower the barriers for biologists to adopt advanced methods and further drive the transition from observation to manipulation in super-resolution microscopy. Label-free techniques, or virtual staining, transform bright field micrographs into fluorescence images with high SNR.[132,133] By computationally measuring the spatial distribution of fluorophores, these methods can recapitulate fluorescence microscopy results without the need for physical staining or labeling, significantly reducing phototoxicity. Finally, the establishment of SIM image databases will be essential for advancing the field, providing valuable resources for researchers to develop new deep learning algorithms based on large-data.[102,134] Moreover, public datasets can serve as a benchmark for evaluating the performance of image processing algorithms and deep learning models.

Taken together, we envision that future advances in SIM technology will not only focus on improving image reconstruction but also on optimizing image acquisition processes. By integrating content-rich outputs and developing module-diverse systems tailored to specific biological activities, smart SIM system will unveil its full potential in the field of cell biology.

Acknowledgements

H.Z. and Y.Z. contributed equally to this work. This work was supported by the National Key Research and Development Program of China (2021YFF0700305), Zhejiang Provincial Natural Science Foundation (Nos. LZ23H180002 and 2024C03056), Zhejiang University K.P.Chao's High Technology Development Foundation (2022RC009), and the Fundamental Research Funds for the Central Universities (226-2024-00059).

Conflict of Interest

The authors declare no conflict of interest.

Keywords

artificial intelligence, deep learning, live-cell imaging, structured illumination microscopy, super-resolution imaging

Received: September 29, 2024
Revised: February 21, 2025
Published online: March 3, 2025

[1] R. Heintzmann, M. G. L. Gustafsson, *Nat. Photonics* **2009**, *3*, 362.
[2] S. J. Sahl, S. W. Hell, S. Jakobs, *Nat. Rev. Mol. Cell Biol.* **2017**, *18*, 685.
[3] Y. Wu, H. Shroff, *Nat. Methods* **2018**, *15*, 1011.
[4] L. Schermelleh, A. Ferrand, T. Huser, C. Eggeling, M. Sauer, O. Biehlmaier, G. P. C. Drummen, *Nat. Cell Biol.* **2019**, *21*, 72.
[5] R. Heintzmann, T. Huser, *Chem. Rev.* **2017**, *117*, 13890.
[6] M. Sivaguru, M. A. Urban, G. Fried, C. J. Wesseln, L. Mander, S. W. Punyasena, *Microsc. Res. Tech.* **2018**, *81*, 101.
[7] M. G. L. Gustafsson, *Proc. Natl. Acad. Sci. USA* **2005**, *102*, 13081.
[8] M. J. Rust, M. Bates, X. Zhuang, *Nat. Methods* **2006**, *3*, 793.
[9] E. Betzig, G. H. Patterson, R. Sougrat, O. W. Lindwasser, S. Olenych, J. S. Bonifacino, M. W. Davidson, J. Lippincott-Schwartz, H. F. Hess, *Science* **2006**, *313*, 1642.
[10] T. A. Klar, S. W. Hell, *Opt. Lett.* **1999**, *24*, 954.
[11] S. W. Hell, *Science* **2007**, *316*, 1153.
[12] R. Fiolka, L. Shao, E. H. Rego, M. W. Davidson, M. G. L. Gustafsson, *Proc. Natl. Acad. Sci. USA* **2012**, *109*, 5311.
[13] D. Li, L. Shao, B.-C. Chen, X. Zhang, M. Zhang, B. Moses, D. E. Milkie, J. R. Beach, J. A. Hammer, M. Pasham, T. Kirchhausen, M. A. Baird, M. W. Davidson, P. Xu, E. Betzig, *Science* **2015**, *349*, aab3500.
[14] Y. Ma, K. Wen, M. Liu, J. Zheng, K. Chu, Z. J. Smith, L. Liu, P. Gao, *J. Phys. Photonics* **2021**, *3*, 024009.
[15] M. G. L. Gustafsson, *J. Microsc.* **2000**, *198*, 82.
[16] A. Forbes, M. de Oliveira, M. R. Dennis, *Nat. Photonics* **2021**, *15*, 253.
[17] T. Zhao, Z. Wang, T. Chen, M. Lei, B. Yao, P. R. Bianco, *Front. Phys.* **2021**, *9*, 672555.
[18] S. J. Sahl, S. W. Hell, in *High Resolution Imaging in Microscopy and Ophthalmology: New Frontiers in Biomedical Optics*, (Ed: J. F. Bille), Springer International Publishing, Cham **2019**, pp. 3.
[19] B.-J. Chang, V. D. Perez Meza, E. H. K. Stelzer, *Proc. Natl. Acad. Sci. USA* **2017**, *114*, 4869.
[20] F. Wang, Z. Ma, Y. Zhong, F. Salazar, C. Xu, F. Ren, L. Qu, A. M. Wu, H. Dai, *Proc. Natl. Acad. Sci. USA* **2021**, *118*, 2023888118.
[21] B. Chen, B.-J. Chang, P. Roudot, F. Zhou, E. Sapoznik, M. Marlar-Pavey, J. B. Hayes, P. T. Brown, C.-W. Zeng, T. Lambert, J. R. Friedman, C.-L. Zhang, D. T. Burnette, D. P. Shepherd, K. M. Dean, R. P. Fiolka, *Nat. Methods* **2022**, *19*, 1419.
[22] R. Fiolka, *Nat. Methods* **2022**, *19*, 1355.
[23] Y. Wang, Z. Yu, C. K. Cahoon, T. Parmely, N. Thomas, J. R. Unruh, B. D. Slaughter, R. S. Hawley, *Nat. Protoc.* **2018**, *13*, 1869.
[24] O. Schulz, C. Pieper, M. Clever, J. Pfaff, A. Ruhlandt, R. H. Kehlenbach, F. S. Wouters, J. Großhans, G. Bunt, J. Enderlein, *Proc. Natl. Acad. Sci. USA* **2013**, *110*, 21000.
[25] F. Ströhl, C. F. Kaminski, *Optica* **2016**, *3*, 667.
[26] E. Ward, R. Pal, *J. Microsc.* **2017**, *266*, 221.
[27] B.-C. Chen, W. R. Legant, K. Wang, L. Shao, D. E. Milkie, M. W. Davidson, C. Janetopoulos, X. S. Wu, J. A. Hammer, Z. Liu, B. P. English, Y. Mimori-Kiyosue, D. P. Romero, A. T. Ritter, J. Lippincott-Schwartz, L. Fritz-Laylin, R. D. Mullins, D. M. Mitchell, J. N. Bembenek, A.-C. Reymann, R. Böhme, S. W. Grill, J. T. Wang, G. Seydoux, U. S. Tulu, D. P. Kiehart, E. Betzig, *Science* **2014**, *346*, 1257998.
[28] C. Zhang, N. Xu, Q. Tan, *Biomed. Opt. Express* **2022**, *13*, 6113.
[29] H.-W. Lu-Walther, M. Kielhorn, R. Förster, A. Jost, K. Wicker, R. Heintzmann, *Methods Appl. Fluoresc.* **2015**, *3*, 014001.
[30] A. Sandmeyer, M. Lachetta, H. Sandmeyer, W. Hübner, T. Huser, M. Müller, *bioarXiv* **2019**.
[31] A. Lal, C. Shan, P. Xi, *IEEE J. Sel. Top. Quantum Electron.* **2016**, *22*, 50.
[32] C.-H. Yeh, S.-Y. Chen, *Appl. Opt.* **2015**, *54*, 2309.
[33] J. Huff, *Nat. Methods* **2015**, *12*, i.
[34] C. J. R. Sheppard, *Appl. Sci.* **2021**, *11*, 8981.
[35] C. Zhang, B. Yu, F. Lin, S. Samanta, H. Yu, W. Zhang, Y. Jing, C. Shang, D. Lin, K. Si, W. Gong, J. Qu, *PhotoniX* **2023**, *4*, 38.
[36] A. G. York, S. H. Parekh, D. D. Nogare, R. S. Fischer, K. Temprine, M. Mione, A. B. Chitnis, C. A. Combs, H. Shroff, *Nat. Methods* **2012**, *9*, 749.
[37] H. An, W. Koh, S. Kang, M.-H. Nam, C. J. Lee, *Exp. Neurobiol.* **2021**, *30*, 213.
[38] G. M. Gibson, S. D. Johnson, M. J. Padgett, *Opt. Express* **2020**, *28*, 28190.
[39] H.-M. Chen, J.-P. Yang, H.-T. Yen, Z.-N. Hsu, Y. Huang, S.-T. Wu, *Appl. Sci.* **2018**, *8*, 2323.
[40] M. Pivnenko, K. Li, D. Chu, *Opt. Express* **2021**, *29*, 24614.
[41] X.-B. Hu, C. Rosales-Guzmán, *J. Opt.* **2022**, *24*, 034001.
[42] E. Mudry, K. Belkebir, J. Girard, J. Savatier, E. Le Moal, C. Nicoletti, M. Allain, A. Sentenac, *Nat. Photonics* **2012**, *6*, 312.
[43] R. Ayuk, H. Giovannini, A. Jost, E. Mudry, J. Girard, T. Mangeat, N. Sandeau, R. Heintzmann, K. Wicker, K. Belkebir, A. Sentenac, *Opt. Lett.* **2013**, *38*, 4723.
[44] J. Idier, S. Labouesse, M. Allain, P. Liu, S. Bourguignon, A. Sentenac, *IEEE Trans. Comput. Imaging* **2018**, *4*, 87.
[45] A. Vigoren, J. M. Zavislan, *J. Opt. Soc. Am. A* **2018**, *35*, 474.
[46] Y. Novikau, R. Wolleschensky, Introducing Lattice SIM for ZEISS Elyra 7-Structured Illumination Microscopy with a 3D Lattice for Live Cell Imaging, https://pages.zeiss.com/rs/896-XMS-794/images/ZEISS-Microscopy-Technology-Note-Introducing-Lattice-SIM.pdf, (accessed: December, 2018).
[47] A. Löschberger, Y. Novikau, R. Netz, M.-C. Spindler, R. Benavente, T. Klein, M. Sauer, D. I. Kleppe, *bioRxiv 12.443720* **2021**.
[48] T. Zhao, Z. Wang, M. Shu, J. Zhang, Y. Liang, S. Wang, M. Lei, *arXiv 2402.02775* **2024**.
[49] J. Fan, X. Huang, L. Li, S. Tan, L. Chen, *Biophys. Rep.* **2019**, *5*, 80.
[50] A. Markwirth, M. Lachetta, V. Mönkemöller, R. Heintzmann, W. Hübner, T. Huser, M. Müller, *Nat. Commun.* **2019**, *10*, 4315.
[51] J. Qian, Y. Cao, Y. Bi, H. Wu, Y. Liu, Q. Chen, C. Zuo, *eLight* **2023**, *3*, 4.
[52] S. Tu, Q. Liu, X. Liu, W. Liu, Z. Zhang, T. Luo, C. Kuang, X. Liu, X. Hao, *Opt. Lett.* **2020**, *45*, 1567.
[53] G. Wen, S. Li, L. Wang, X. Chen, Z. Sun, Y. Liang, X. Jin, Y. Xing, Y. Jiu, Y. Tang, H. Li, *Light: Sci. Appl.* **2021**, *10*, 70.
[54] Z. Wang, T. Zhao, H. Hao, Y. Cai, K. Feng, X. Yun, Y. Liang, S. Wang, Y. Sun, P. R. Bianco, K. Oh, M. Lei, *Adv. Photonics* **2022**, *4*, 026003.
[55] Z. Wang, T. Zhao, Y. Cai, J. Zhang, H. Hao, Y. Liang, S. Wang, Y. Sun, T. Chen, P. R. Bianco, K. Oh, M. Lei, *Innovation* **2023**, *4*, 100425.
[56] Y. Mo, K. Wang, L. Li, S. Xing, S. Ye, J. Wen, X. Duan, Z. Luo, W. Gou, T. Chen, Y.-H. Zhang, C. Guo, J. Fan, L. Chen, *Nat. Commun.* **2023**, *14*, 3089.
[57] J. Qian, K. Xu, S. Feng, Y. Liu, H. Ma, Q. Chen, C. Zuo, *ACS Photonics* **2024**, *11*, 1887.

[58] X. Huang, J. Fan, L. Li, H. Liu, R. Wu, Y. Wu, L. Wei, H. Mao, A. Lal, P. Xi, L. Tang, Y. Zhang, Y. Liu, S. Tan, L. Chen, *Nat. Biotechnol.* **2018**, *36*, 451.
[59] W. Zhao, S. Zhao, L. Li, X. Huang, S. Xing, Y. Zhang, G. Qiu, Z. Han, Y. Shang, D. Sun, C. Shan, R. Wu, L. Gu, S. Zhang, R. Chen, J. Xiao, Y. Mo, J. Wang, W. Ji, X. Chen, B. Ding, Y. Liu, H. Mao, B.-L. Song, J. Tan, J. Liu, H. Li, L. Chen, *Nat. Biotechnol.* **2022**, *40*, 606.
[60] A. Lal, C. Shan, K. Zhao, W. Liu, X. Huang, W. Zong, L. Chen, P. Xi, *IEEE Trans. Image Process.* **2018**, *27*, 4555.
[61] Y. Zhang, J. Fei, G. Liu, J. Deng, H. Yang, *OSA Continuum, OSAC* **2020**, *3*, 1.
[62] J. Qian, Y. Cao, K. Xu, Y. Bi, W. Xia, Q. Chen, C. Zuo, *Appl. Phys. Lett.* **2022**, *121*, 153701.
[63] H. Wu, Y. Li, Y. Sun, L. Yin, W. Sun, Z. Ye, X. Yang, H. Zhu, M. Tang, Y. Han, C. Kuang, X. Liu, *APL Photonics* **2024**, *9*, 036102.
[64] Y. Guo, D. Li, S. Zhang, Y. Yang, J.-J. Liu, X. Wang, C. Liu, D. E. Milkie, R. P. Moore, U. S. Tulu, D. P. Kiehart, J. Hu, J. Lippincott-Schwartz, E. Betzig, D. Li, *Cell* **2018**, *175*, 1430.
[65] M. Tokunaga, N. Imamoto, K. Sakata-Sogawa, *Nat. Methods* **2008**, *5*, 159.
[66] M. Weigert, U. Schmidt, T. Boothe, A. Müller, A. Dibrov, A. Jain, B. Wilhelm, D. Schmidt, C. Broaddus, S. Culley, M. Rocha-Martins, F. Segovia-Miranda, C. Norden, R. Henriques, M. Zerial, M. Solimena, J. Rink, P. Tomancak, L. Royer, F. Jug, E. W. Myers, *Nat. Methods* **2018**, *15*, 1090.
[67] X. Li, Y. Wu, Y. Su, I. Rey-Suarez, C. Matthaeus, T. B. Updegrove, Z. Wei, L. Zhang, H. Sasaki, Y. Li, M. Guo, J. P. Giannini, H. D. Vishwasrao, J. Chen, S.-J. J. Lee, L. Shao, H. Liu, K. S. Ramamurthi, J. W. Taraska, A. Upadhyaya, P. La Riviere, H. Shroff, *Nat. Biotechnol.* **2023**, *41*, 1307.
[68] Z. Ouyang, Q. Wang, X. Li, Q. Dai, M. Tang, L. Shao, W. Gou, Z. Yu, Y. Chen, B. Zheng, L. Chen, C. Ping, X. Bi, B. Xiao, X. Yu, C. Liu, L. Chen, J. Fan, X. Huang, Y. Zhang, *Nat. Methods* **2024**, *22*, 335.
[69] L. Shao, B. Isaac, S. Uzawa, D. A. Agard, J. W. Sedat, M. G. L. Gustafsson, *Biophys. J.* **2008**, *94*, 4971.
[70] E. He, Y. Sun, H. Zhu, X. Yang, L. Yin, Y. Han, C. Kuang, X. Liu, *arXiv* **2025**, 629092.
[71] C. S. Smith, J. A. Slotman, L. Schermelleh, N. Chakrova, S. Hari, Y. Vos, C. W. Hagen, M. Müller, W. van Cappellen, A. B. Houtsmuller, J. P. Hoogenboom, S. Stallinga, *Nat. Methods* **2021**, *18*, 821.
[72] A. Bilodeau, C. V. L. Delmas, M. Parent, P. De Koninck, A. Durand, F. Lavoie-Cardinal, *Nat. Mach. Intell.* **2022**, *4*, 455.
[73] Z. Liu, L. Jin, J. Chen, Q. Fang, S. Ablameyko, Z. Yin, Y. Xu, *Comput. Biol. Med.* **2021**, *134*, 104523.
[74] C. Qiao, D. Li, Y. Liu, S. Zhang, K. Liu, C. Liu, Y. Guo, T. Jiang, C. Fang, N. Li, Y. Zeng, K. He, X. Zhu, J. Lippincott-Schwartz, Q. Dai, D. Li, *Nat. Biotechnol.* **2022**, *41*, 367.
[75] O. Ronneberger, P. Fischer, T. Brox, in *Medical Image Computing and Computer-Assisted Intervention – MICCAI 2015*, (Eds.: N. Navab, J. Hornegger, W.M. Wells, A. F. Frangi), Springer International Publishing, Cham **2015**, pp. 234.
[76] Y. Zhang, K. Li, K. Li, L. Wang, B. Zhong, Y. Fu, *Proceedings of the European Conference on Computer Vision (ECCV)*, Springer, Berlin **2018**, pp. 286–301.
[77] F. Luo, J. Zeng, Z. Shao, C. Zhang, *Optics Lasers Eng.* **2023**, *162*, 107432.
[78] D. Mahecic, W. L. Stepp, C. Zhang, J. Griffié, M. Weigert, S. Manley, *Nat. Methods* **2022**, *19*, 1262.
[79] Q. Zhang, J. Chen, J. Li, E. Bo, H. Jiang, X. Lu, L. Zhong, J. Tian, *Optics Lasers Eng.* **2022**, *155*, 107066.
[80] L. Jin, B. Liu, F. Zhao, S. Hahn, B. Dong, R. Song, T. C. Elston, Y. Xu, K. M. Hahn, *Nat. Commun.* **2020**, *11*, 1934.
[81] Z. H. Shah, M. Müller, T.-C. Wang, P. M. Scheidig, A. Schneider, M. Schüttpelz, T. Huser, W. Schenck, *Photonics Res.* **2021**, *9*, B168.
[82] X. Zhu, X. Chang, R. Zhao, Z. Wu, S. Wang, Q. Jiao, L. Bian, in *Optoelectronic Imaging and Multimedia Technology*, IX, SPIE, Bellingham, WA **2023**, pp. 47–53.
[83] B. Liu, J. Liao, Y. Song, C. Chen, L. Ding, J. Lu, J. Zhou, F. Wang, *Nanoscale Adv.* **2021**, *4*, 30.
[84] C. Ling, C. Zhang, M. Wang, F. Meng, L. Du, X. Yuan, *Photonics Res.* **2020**, *8*, 1350.
[85] H. Wang, Y. Rivenson, Y. Jin, Z. Wei, R. Gao, H. Günaydın, L. A. Bentolila, C. Kural, A. Ozcan, *Nat. Methods* **2019**, *16*, 103.
[86] C. Qiao, X. Chen, S. Zhang, D. Li, Y. Guo, Q. Dai, D. Li, *IEEE J. Sel. Top. Quantum Electron.* **2021**, *27*, 1.
[87] P. Wijesinghe, S. Corsetti, D. J. X. Chow, S. Sakata, K. R. Dunning, K. Dholakia, *Light: Sci. Appl.* **2022**, *11*, 319.
[88] X. Chen, B. Li, S. Jiang, T. Zhang, X. Zhang, P. Qin, X. Yuan, Y. Zhang, G. Zheng, X. Ji, *IEEE Trans. Comput. Imag.* **2021**, *7*, 700.
[89] Y. He, Y. Yao, Y. He, Z. Huang, F. Luo, C. Zhang, D. Qi, T. Jia, Z. Wang, Z. Sun, X. Yuan, S. Zhang, *Biomed. Opt. Express* **2023**, *14*, 106.
[90] X. Liu, J. Li, X. Fang, J. Li, J. Zheng, J. Li, N. Ali, C. Zuo, P. Gao, S. An, *Opt. Commun.* **2023**, *537*, 129431.
[91] Z. Burns, Z. Liu, *Opt. Express* **2023**, *31*, 8714.
[92] S. Dong, J. Liao, K. Guo, L. Bian, J. Suo, G. Zheng, *Biomed. Opt. Express* **2015**, *6*, 2946.
[93] F. Orieux, E. Sepulveda, V. Loriette, B. Dubertret, J.-C. Olivo-Marin, *IEEE Trans. Image Process.* **2012**, *21*, 601.
[94] J.-Y. Zhu, T. Park, P. Isola, A. A. Efros, presented at 2017 IEEE International Conference on Computer Vision (ICCV), Venice, Italy, (accessed: October 2017).
[95] C. Ling, L. Du, X. Yuan, in *AOPC 2020: Display Technology; Photonic MEMS, THz MEMS, and Metamaterials; and AI in Optics and Photonics*, SPIE, Bellingham, WA **2020**, pp. 138–143.
[96] M. Mirza, S. Osindero, *arXiv* **2014**, 1784.
[97] X. Cheng, J. Li, Q. Dai, Z. Fu, J. Yang, *IEEE Trans. Instrum. Meas.* **2022**, *71*, 5007711.
[98] S. Yang, B.-U. Lee, *PLoS One* **2015**, *10*, 0136964.
[99] A. K. Boyat, B. K. Joshi, presented at 2014 IEEE International Conference on Computational Intelligence and Computing Research, Coimbatore, India, (accessed: December 2014).
[100] W. H. Richardson, *J. Opt. Soc. Am.* **1972**, *62*, 55.
[101] L. B. Lucy, *Astronomical J.* **1974**, *79*, 745.
[102] C. Qiao, D. Li, Y. Guo, C. Liu, T. Jiang, Q. Dai, D. Li, *Nat. Methods* **2021**, *18*, 194.
[103] E. Xypakis, G. Gosti, T. Giordani, R. Santagati, G. Ruocco, M. Leonetti, *Sci. Rep.* **2022**, *12*, 8623.
[104] Y. Chen, Q. Liu, J. Zhang, Z. Ye, H. Ye, Y. Zhu, C. Kuang, Y. Chen, W. Liu, *Opt. Express* **2024**, *32*, 3316.
[105] X. Chen, C. Qiao, T. Jiang, J. Liu, Q. Meng, Y. Zeng, H. Chen, H. Qiao, D. Li, J. Wu, *PhotoniX* **2024**, *5*, 4.
[106] H. Wang, Y. Rivenson, Y. Jin, Z. Wei, R. Gao, H. Günaydın, L. A. Bentolila, C. Kural, A. Ozcan, in *Biophotonics Congress: Biomedical Optics 2020 (Translational, Microscopy, OCT, OTS, BRAIN)*, Optica Publishing Group, Massachusetts, Washington **2020**, p. MM3A4.
[107] C. Sun, A. Shrivastava, S. Singh, A. Gupta, presented at 2017 IEEE International Conference on Computer Vision (ICCV), Venice, Italy, (accessed: December 2017).
[108] C. N. Christensen, E. N. Ward, M. Lu, P. Lio, C. F. Kaminski, *Biomed. Opt. Express* **2021**, *12*, 2720.
[109] E. Agustsson, R. Timofte, presented at 2017 IEEE Conference on Computer Vision and Pattern Recognition Workshops, Honolulu, HI, USA, (accessed: July 2017).

[110] E. N. Ward, L. Hecker, C. N. Christensen, J. R. Lamb, M. Lu, L. Mascheroni, C. W. Chung, A. Wang, C. J. Rowlands, G. S. K. Schierle, C. F. Kaminski, *Nat. Commun.* **2022**, *13*, 7836.
[111] J. Wang, J. Fan, B. Zhou, X. Huang, L. Chen, *Adv. Photonics Nexus* **2023**, *2*, 016012.
[112] T. Liu, J. Niu, J. Liu, D. Li, S. Tan, *Optics Lasers Eng.* **2024**, *173*, 107913.
[113] I. Goodfellow, J. Pouget-Abadie, M. Mirza, B. Xu, D. Warde-Farley, S. Ozair, A. Courville, Y. Bengio, *Commun. ACM* **2020**, *63*, 139.
[114] S. Helgadottir, B. Midtvedt, J. Pineda, A. Sabirsh, C. B. Adiels, S. Romeo, D. Midtvedt, G. Volpe, *Biophys. Rev.* **2021**, *2*, 031401.
[115] X. Liu, J. Li, J. Li, N. Ali, T. Zhao, S. An, J. Zheng, Y. Ma, J. Qian, C. Zuo, P. Gao, *Opt. Laser Technol.* **2024**, *170*, 110224.
[116] J. Demmerle, C. Innocent, A. J. North, G. Ball, M. Müller, E. Miron, A. Matsuda, I. M. Dobbie, Y. Markaki, L. Schermelleh, *Nat. Protoc.* **2017**, *12*, 988.
[117] J. Lehtinen, J. Munkberg, J. Hasselgren, S. Laine, T. Karras, M. Aittala, T. Aila, in Proceedings of the 35th International Conference on Machine Learning, PMLR, NY, USA **2018**, pp. 2965–2974.
[118] Y. Li, Y. Su, M. Guo, X. Han, J. Liu, H. D. Vishwasrao, X. Li, R. Christensen, T. Sengupta, M. W. Moyle, I. Rey-Suarez, J. Chen, A. Upadhyaya, T. B. Usdin, D. A. Colón-Ramos, H. Liu, Y. Wu, H. Shroff, *Nat. Methods* **2022**, *19*, 1427.
[119] A. Singh, S. Sengupta, V. Lakshminarayanan, *J. Imag.* **2020**, *6*, 52.
[120] M. T. M. Hannebelle, E. Raeth, S. M. Leitao, T. Lukeš, J. Pospíšil, C. Toniolo, O. F. Venzin, A. Chrisnandy, P. P. Swain, N. Ronceray, M. P. Lütolf, A. C. Oates, G. M. Hagen, T. Lasser, A. Radenovic, J. D. McKinney, G. E. Fantner, *Nat. Commun.* **2024**, *15*, 1550.
[121] R. F. Laine, G. Goodfellow, L. J. Young, J. Travers, D. Carroll, O. Dibben, H. Bright, C. F. Kaminski, *eLife* **2018**, *7*, 40183.
[122] A. Vaswani, N. Shazeer, N. Parmar, J. Uszkoreit, L. Jones, A. N. Gomez, Ł. Kaiser, I. Polosukhin, in *Advances in Neural Information Processing Systems*, Curran Associates Inc, Red Hook, NY, USA **2017**, pp. 6000–6010.
[123] A. Dosovitskiy, L. Beyer, A. Kolesnikov, D. Weissenborn, X. Zhai, T. Unterthiner, M. Dehghani, M. Minderer, G. Heigold, S. Gelly, J. Uszkoreit, N. Houlsby, *arXiv* **2020**.
[124] Z. H. Shah, M. Müller, W. Hübner, T.-C. Wang, D. Telman, T. Huser, W. Schenck, *GigaScience* **2024**, *13*, giad109.
[125] Y. Zheng, J. Chen, C. Wu, W. Gong, K. Si, *Cytometry, Part A* **2021**, *99*, 622.
[126] T. Woo, S. H. Jung, C. Ahn, B. Hwang, H. Kim, J. H. Kang, J.-H. Park, *Optica* **2020**, *7*, 973.
[127] M.-A. Bray, S. Singh, H. Han, C. T. Davis, B. Borgeson, C. Hartland, M. Kost-Alimova, S. M. Gustafsdottir, C. C. Gibson, A. E. Carpenter, *Nat. Protoc.* **2016**, *11*, 1757.
[128] N. Moshkov, M. Bornholdt, S. Benoit, M. Smith, C. McQuin, A. Goodman, R. A. Senft, Y. Han, M. Babadi, P. Horvath, B. A. Cimini, A. E. Carpenter, S. Singh, J. C. Caicedo, *Nat. Commun.* **2022**, *15*, 1594.
[129] N. Cerisier, B. Dafniet, A. Badel, O. Taboureau, *Toxicol. Appl. Pharmacol.* **2023**, *461*, 116407.
[130] R. Diekmann, D. L. Wolfson, C. Spahn, M. Heilemann, M. Schüttpelz, T. Huser, *Nat. Commun.* **2016**, *7*, 13711.
[131] D. Gong, C. Cai, A. Ashesh, G. Schlafly, P. J. L. Rivière, F. Jug, J. Chen, N. F. Scherer, in *Three-Dimensional and Multidimensional Microscopy: Image Acquisition and Processing*, XXXI, SPIE, Bellingham, WA **2024**, p. PC128480N.
[132] C. Ounkomol, S. Seshamani, M. M. Maleckar, F. Collman, G. R. Johnson, *Nat. Methods* **2018**, *15*, 917.
[133] Y. Jo, H. Cho, W. S. Park, G. Kim, D. Ryu, Y. S. Kim, M. Lee, S. Park, M. J. Lee, H. Joo, H. Jo, S. Lee, S. Lee, H. Min, W. D. Heo, Y. Park, *Nat. Cell Biol.* **2021**, *23*, 1329.
[134] E. Williams, J. Moore, S. W. Li, G. Rustici, A. Tarkowska, A. Chessel, S. Leo, B. Antal, R. K. Ferguson, U. Sarkans, A. Brazma, R. E. Carazo Salas, J. R. Swedlow, *Nat. Methods* **2017**, *14*, 775.

Heng Zhang received his B.S. degree in 2021 in biomedical engineering from University of Shanghai for Science and Technology, and M.S. degree in 2024 in biomedical engineering from Zhejiang University. His research focuses on super-resolution florescent microscopy.

Yunqi Zhu received his B.S. degree in 2022 in biomedical engineering from Zhejiang University. He is now a Ph.D. student under the supervision of Prof. Yingke Xu in Zhejiang University. His current research focuses on super-resolution florescent microscopy and deep-learning based medical imaging processing.

Xu Liu received his D.Sc. from L'Ecole Nationale Supérieure de Physiquede Marseille in France. He has been a professor at the College of Optical Science and Engineering, Zhejiang University since 1995. His research interests include optoelectronic display, optics and optoelectronic thin films, optical imaging, and biooptical technologies.

Yingke Xu received the Ph.D. degree in biomedical engineering from Zhejiang University in 2008. From 2008 to 2012, he worked with Yale University as a postdoctoral associate and then was promoted to an associate research scientist. He started his independent research group with the Department of Biomedical Engineering, Zhejiang University in 2012, where he is currently a professor of biomedical engineering and the assistant dean of the College of Biomedical Engineering and Instrument Science. His research interests include biophotonics, optical imaging, image processing, and medical device.